LBL-31276
Preprint

Lawrence Berkeley Laboratory
UNIVERSITY OF CALIFORNIA

Submitted to Nuclear Instruments and Methods A

High Resolution Multiparticle Tracking without Preprocessing via Elastic Tracking

M. Gyulassy and M. Harlander

November 1991

LOAN COPY
Circulates
for 4 weeks
Bldg. 50 Library.
LBL-31276
Copy 2

Prepared for the U.S. Department of Energy under Contract Number DE-AC03-76SF00098

DISCLAIMER

This document was prepared as an account of work sponsored by the United States Government. While this document is believed to contain correct information, neither the United States Government nor any agency thereof, nor the Regents of the University of California, nor any of their employees, makes any warranty, express or implied, or assumes any legal responsibility for the accuracy, completeness, or usefulness of any information, apparatus, product, or process disclosed, or represents that its use would not infringe privately owned rights. Reference herein to any specific commercial product, process, or service by its trade name, trademark, manufacturer, or otherwise, does not necessarily constitute or imply its endorsement, recommendation, or favoring by the United States Government or any agency thereof, or the Regents of the University of California. The views and opinions of authors expressed herein do not necessarily state or reflect those of the United States Government or any agency thereof or the Regents of the University of California.

LBL-31276

High Resolution Multiparticle Tracking without Preprocessing via Elastic Tracking*

Miklos Gyulassy and Magnus Harlander[1]

Nuclear Science Division
Lawrence Berkeley Laboratory
Berkeley, CA 94720 USA

Abstract:
Elastic Tracking (ET) is applied to the problem of tracking noisy overlapping tracks in visual and electronic detectors. The method avoids the necessity of local preprocessing to find track centroids and utilizes global information provided by the detector to resolve small momentum differences between multiple overlapping tracks for applications such as pion interferometry.

PACS: 6.50.-x, 29.80.-j, 89.90.+c

1 Introduction

Recently we proposed a new method[1], called Elastic Tracking (ET), to extend tracking capabilities to much higher track densities than previously possible with conventional methods[2, 3, 4]. The track density, ρ_{track}, defined here by the ratio of the average distance between measured points along a track to the average distance between tracks provides a convenient measure of the complexity of a given tracking task. Conventional methods typically break down near $\rho_{track} \sim 1$, when the ionization distribution produced by adjacent tracks begin to overlap significantly. In Ref.[1] we showed that ET can resolve tracks in high multiplicity events at densities up to $\rho_{track} \sim 10$ even in the presence of 100% noise! The power of the method stems from the use of *global* information on the ionization charge density provided by the detector together with the known physical characteristics of valid trajectories in that detector. ET is based on a generalization of the familiar Radon or Hough transform[2] as an effective interaction energy of an elastic distribution of charge in

[0]*This work was supported by the Director, Office of Energy Research, Division of Nuclear Physics of the Office of High Energy and Nuclear Physics of the U.S. Department of Energy under Contract No. DE-AC03-76SF00098.

[1]Permanent address: Technische Univ. München, Physics Department T30, James Franck Strasse 1, 8046 Garching, Germany.

a field produced by the measured ionization charge density. It is a generalization of Elastic Network algorithms[5] used to solve geometrical optimization problems via a system of dynamical equations. In Ref.[6] an alternate generalization of Elastic Networks was proposed using deformable templates and deterministic annealing. In ET adaptive tracking and fitting are performed simultaneously by solving dynamical equations of motion of elastic *distributions* of charge. The global minimum of the ET energy functional is found by introducing a slowly decreasing range for the effective potential. The unique aspect of the ET algorithm that we focus on in this work is its ability to utilize directly the "raw" ionization density measured by the detector, thereby eliminating the need for and the limitation imposed by extensive local preprocessing of the data.

In high energy particle and nuclear physics, a common problem is the measurement of high multiplicity events in detectors such as as a bubble, streamer, or time projection chambers in which particle trajectories are constrained by known electric and magnetic fields (see e.g. [7, 8, 9]). The pattern recognition problem involved in tracking is simplified in this case by the knowledge of the class of all possible trajectories in the detector. We denote those trajectories by

$$\mathbf{r}_\phi(\tau), \text{ where } \phi \equiv \{\mathbf{x}, \mathbf{p}\} \text{ and } \mathbf{r}_\phi(0) = \mathbf{x},\ d\mathbf{r}_\phi(0)/d\tau = \mathbf{p}/m \ , \tag{1}$$

for a particle of mass m, produced at vertex position, $\mathbf{x}$, with momentum, $\mathbf{p}$. We assume that $\mathbf{r}_\phi(\tau)$ is either known analytically, e.g., helices in a uniform magnetic field, or computable numerically from the known equations of motion, $m dp^\mu/d\tau = eF^{\mu\nu}_{ex} p_\nu$, in the external EM field, $F^{\mu\nu}_{ex}(x)$, within the detector.

Given N tracks specified by the phase space points $\phi_\alpha = \{\mathbf{x}_\alpha, \mathbf{p}_\alpha\}$, we assume that the output of the detector is an amplified source ionization density,

$$\rho_S(\mathbf{x}) = \sum_\alpha \rho_\alpha(\mathbf{x}) \ , \tag{2}$$

where the density induced by track α is expressed as

$$\rho_\alpha(\mathbf{x}) = \int d\tau q(\mathbf{r}_\alpha(\tau))\sigma(\mathbf{x} - \mathbf{r}_\alpha(\tau)) \ , \tag{3}$$

with $q(\mathbf{r}_\alpha(\tau))$ being proportional to the variable ionization charge density along the track. The finite range distribution, $\sigma(\mathbf{x})$, depends on the characteristics of the detector. On the average $\langle q \rangle$ is assumed to be proportional to the mean dE/dx of the particle. However, in physical detectors, Landau fluctuations[10] cause large local fluctuations of q around that mean. In general, the width of $\sigma(\mathbf{x})$ also fluctuates along the track, but we restrict the present study to the influence of charge fluctuations alone.

The conventional approach to tracking begins with a preprocessing stage in which the detector is segmented into rows of width Δz and mean centroids, $\mathbf{x}_{k\alpha} = \{\langle \mathbf{x}_\perp \rangle_\alpha, k\Delta z\}$ of distributed charges are estimated locally on each row k. After this preprocessing stage the ionization charge density is approximated by

$$\rho(\mathbf{x}) = -\langle q \rangle \sum_{k,\alpha} \delta(\mathbf{x} - \mathbf{x}_{k\alpha}) \ . \tag{4}$$

In Ref.[1] we studied extensively the tracking problem given such preprocessed distributions. We showed that conventional local tracking algorithms such as Road Finder (RF)[4] break down for $\rho_{track} \gtrsim 1$ and even the novel neural-network Denby-Peterson (DP) algorithm[11, 12] broke down for $\rho_{track} \gtrsim 5$. On the other hand, the ET algorithm continued to perform well up to $\rho_{track} \sim 10$.

However, it is clear that local preprocessing of the data is itself a major limiting factor in achieving the highest possible tracking resolution because valuable global information is lost when the data are reduced on each layer separately. In particular, in the case of overlapping tracks, the local fluctuating charge deposition from row to row makes it difficult to estimate the track centroids accurately. Obviously, a global strategy that avoids this preprocessing stage should be able to reach significantly higher resolution on two track separations. In Ref.[1], we emphasized that ET in fact provides such a global strategy since it can deal in principal directly with continuous data $\rho_S(x)$. In this work we utilize this capability to address the physically interesting problem of tracking particles with small relative momentum difference leading to overlapping ionization distributions.

Figures 1 and 2 illustrate the type of tracking problems that we consider in this paper. The magnitude of the pad readout of the local ionization density in a 2-D simulation of a TPC-like detector is indicated by the relative size of the solid squares. The detailed discussion of the simulation and results are presented in section 4. Here these examples suffice to illustrate the tracking information on each pad row separately can become locally ambiguous while the global picture can remain clear. As in all pattern recognition problems local ambiguity can only be circumvented by algorithms taking into account the non-local (long range) correlations present in the data. The lines corresponding to the ET solutions show the power of this algorithm to utilize that information.

An important motivation for the present paper is the need to resolve tracks with very small momentum differences in ultrarelativistic nuclear reactions[8, 9]. In that case the physics objectives is to determine reaction zone times and distances on a scale ~ 100 fm/c by studying carefully the multi pion interference pattern resulting from Bose symmetrization. To reduce effects due to Coulomb final state interactions it may be even necessary to resolve 3 or more overlapping mixed charge tracks with small relative momentum[13]. Present conservative estimates[9] based on conventional Road Finding algorithms apparently limit the two particle relative momentum to $\gtrsim 5 - 20$ MeV/c depending on the pion momenta. This limit arises because of the restriction that local preprocessing of centroids requires a track separation of at least 3 pad widths. In this paper we show that significantly better resolution ($\sim \frac{1}{2}$ pad width track separation) can be obtained using the Elastic Tracking algorithm when applied directly to the unprocessed ionization distribution.

The discussion is organized as follows: In section 2, we review the ET algorithm emphasizing its formulation for continuous distributions. A 1-D analytical model is analyzed in section 3 to illustrate how charge fluctuations induce tracking errors and limit the two track resolution. In section 4 numerical results are presented of a more realistic 2-D simulation of ET tracking given image charge distributions characteristic of TPC-like detectors. The relative track resolution is studied as a function of the

opening angle between the tracks and the segmentation of the detector. A summary is presented in section 5.

2 Elastic Tracking

ET is an adaptive template matching algorithm formulated in terms of dynamical systems. The templates are charge distributions parametrized in terms of the class of allowed trajectories, $\mathbf{r}_\phi(\tau)$. For a every allowed phase space point, $\phi_T = \{\mathbf{x}_T, \mathbf{p}_T\}$, we associate a template charge density as follows:

$$\rho_T(\mathbf{x}) = q_T \int d\tau \sigma_T(\mathbf{x} - \mathbf{r}_{\phi_T}(\tau)) \ , \tag{5}$$

where q_T is the charge assigned to that template and where $\sigma_T(\mathbf{x})$ characterizes the shape of the template distribution around the trajectory $\mathbf{r}_{\phi_T}(\tau)$. For M templates, the total template charge density is simply the sum over the density of each.

Tracking in ET is performed by minimizing an effective energy for the combined source and template configuration

$$\rho(\mathbf{x}) = \sum_{\alpha=1}^{N} \rho_\alpha(\mathbf{x}) + \sum_{i=1}^{M} \rho_{T_i}(\mathbf{x}) \ . \tag{6}$$

The ET energy or cost function, $E(t)$, is simply a generalized "Coulomb" energy

$$E(t) = \tfrac{1}{2} \int dx dx' \rho(\mathbf{x}) V(\mathbf{x} - \mathbf{x}', t) \rho(\mathbf{x}') \ , \tag{7}$$

where $V(\mathbf{x}, t)$ is a finite range potential with a range that decreases slowly as a function of the *iteration* time. Any convenient finite range positive definite form can be used for the potential, e.g.,

$$V(\mathbf{x}, t) \propto \exp(-x^2/2w^2(t)) \ , \tag{8}$$

with

$$w(t) = (w_0 - w_f)e^{-\gamma t} + w_f \ . \tag{9}$$

As noted in [1], E reduces to the familiar Radon transform[2] in the limit $V(\mathbf{x}, t) = \delta(\mathbf{x})$ and $\sigma_T(\mathbf{x}) = \delta(\mathbf{x})$. For a static square well potential E reduces essentially to the Hough transform. It is also clear that $E(t) \geq 0$ and that E reaches its minimum, $E = 0$, when the source and template densities overlap and the total charge density is neutralized ($\rho = 0$). This requires of course that the number of templates is identical to the number of tracks, the shape of the templates coincides with that of the source, and that their charge is exactly opposite.

The standard gradient descent method

$$\begin{aligned} d\mathbf{p}_i/dt &= -\eta \nabla_{\mathbf{p}_i} E(t) \ , \\ d\mathbf{x}_i/dt &= -\eta \nabla_{\mathbf{x}_i} E(t) \ , \end{aligned} \tag{10}$$

where η is a small rate parameter is used to define a set of coupled dynamical equations to perform the ET minimization task. Starting from a random initial phase space point $\{(\mathbf{x}_i(0), \mathbf{p}_i(0)),\ i = 1, M\}$, the above equations evolve the phase space point specifying the templates to one of the nearby minima of the interaction energy.

As in all optimization methods care must be taken to avoid getting caught in one of the many *local* minima of the energy surface. The strategy adopted in ET is the introduction of a slowly decreasing range, $w(t)$, of the effective potential as in eq.(9). The initial range, w_0, should be taken to be large as compared with the average width of the measured distribution for an isolated track. The final width, w_f, should be less than that average width. The rate γ needs to be small compared to η so that (10) evolves adiabatically towards the global minimum. In the absence of fluctuations, i.e., $q(\mathbf{r}_\phi(\tau)) = \langle q \rangle$, the above algorithm always converges to the global minimum if $q_T = -\langle q \rangle$ and $\sigma_T = \sigma$.

We note several essential differences between the ET method[1] and the deformable template (DT) algorithm proposed in Ref.[6]. The most important difference in connection with the present application is that ET is formulated to perform tracking given an arbitrary source *distribution*, $\rho_S(x)$, not limited to the form (4). The DT method in its present form is limited to tracking only preprocessed distributions of the form (4). For well separated tracks at low density this difference is not essential since local preprocessing can then be done easily. However, for high density or overlapping tracks, preprocessing is itself problematical and in that case the continuous formulation of ET is advantageous. There is also a technical difference in the strategy used to avoid local minima. In DT deterministic annealing plays the same role as the time dependent range of the ET method. However, the ET approach is more easily customized to specific tracking tasks because the strength and form of the relative and external potentials can be separately varied. For example in [1], the relative template potentials were set to zero, and the template tracks evolved only in the external field generated by the ionization density. This reduces the computational effort in finding well separated tracks. Charge neutralization was achieved by eliminating all data points in a predefined range of the final template density. However, such a neutralization scheme would throw out data in the case of nearly overlapping tracks and thus is not suitable for the present application. In this work the same potential is used between template and source distributions. Charge neutralization is then achieved naturally through balancing the relative and external forces on all templates. In applications to very high multiplicity tracking as in [9] a hybrid approach may be computationally advantageous. For example, the template charge could be set $q_T = 0$ during the first phase of the analysis to minimize the computation while catching most of the non-overlapping tracks. Then the template charge could be turned on to split the rare overlapping track regions.

3 Tracking Errors Due to Charge Fluctuations

Without fluctuations the ET algorithm is in principle exact since the $\rho(x) = 0$ configuration exists. With fluctuating source charges, however, ET can at best only find the

correct track configurations on the average. The rms fluctuations of those parameters arise because for fixed template charges the total charge density cannot be exactly neutralized. This is the basic source of relative tracking error which we analyze in detail below.

To see analytically how such tracking errors arise, we consider in this section the simplest possible one dimensional problem corresponding to tracking two parallel tracks separated by a distance $d = |d_1 - d_2|$. For the source and template density we take

$$\begin{aligned} \rho_S(x) &= q_1\sigma(x-d_1) + q_2\sigma(x-d_2) \ , \\ \rho_T(x) &= \sigma(x-x_1) + \sigma(x-x_2) \ . \end{aligned} \tag{11}$$

The energy is then given by

$$\begin{aligned} E &= \tfrac{1}{2}(q_1^2+q_2^2+2)A(0) + q_1q_2A(d_1-d_2) + A(x_1-x_2) \\ &\quad + q_1(A(x_1-d_1)+A(x_2-d_1)) + q_2(A(x_1+d_2)+A(x_2+d_2)) \ , \end{aligned} \tag{12}$$

where

$$A(x-y) = \int dx'dy'\sigma(x'-x)V(x'-y')\sigma(y'-y) \ .$$

Defining $F(x) = -dA(x)/dx$, the forces on the templates are given by

$$\begin{aligned} F_1(x_1,x_2) &= q_1F(x_1-d_1) + q_2F(x_1-d_2) + F(x_1-x_2) \ , \\ F_2(x_1,x_2) &= q_1F(x_2-d_1) + q_2F(x_2-d_2) - F(x_1-x_2) \ . \end{aligned} \tag{13}$$

We assume that $\sigma(x) = \sigma(-x)$, so that $F(0) = 0$ and $F(-x) = -F(x)$. For the average ionization charge $q_i = -1$, the force on the templates obviously vanishes when they overlap the external distribution at $(x_1, x_2) = \pm(d_1, d_2)$.

For small fluctuations, $q_i = -1 + \delta q_i$, with $\langle \delta q_i \rangle = 0$ and $\langle \delta q_i^2 \rangle = \delta q^2$, we can expand (13) with $x_i = d_i + \delta x_i$, and find that $\langle x_1 - x_2 \rangle = d_1 - d_2$ as expected and that the rms error on the source separation is

$$\Delta d^2 = \langle (x_1-x_2)^2 \rangle - (d_1-d_2)^2 \approx 2\delta q^2 (F(2d)/F'(0))^2 \ . \tag{14}$$

For large fluctuations and short separations the linearized approximation breaks down and the solutions of $F_i = 0$ must be determined numerically. In order to understand the general nonperturbative features of the numerical simulations in the next section, consider $\sigma(x) \propto \exp(-x^2/2)$ such that

$$A(x) = \exp(-x^2/2w^2) \ , \tag{15}$$

where $w^2 = 2 + w_f^2$. Even for this extremely simplified case the zero trajectory curves, $x_2^i(x_1)$, which solve $F_i(x_1, x_2^i(x_1)) = 0$, are found to wind and weave back and forth around each other with several intersections in the (x_1, x_2) plane for a fixed q_i, d_i. Template exchange symmetry leads to a two fold degeneracy of extrema. In the case of well separated tracks but not too large charge fluctuations, in addition to the true

global minimum at $(x_1, x_2) \approx (d_1, d_2)$ (and (d_2, d_1)) there are two local minima with $(x_1, x_2) \approx (d_i + \delta, d_i - \delta)$ corresponding to a bound state of two templates around each of the isolated sources.

When the charge fluctuations exceed a certain value, however, there is an interesting phase transition in this system. In Fig.3 we show the final template density corresponding to the global minimum of the interaction energy for different source charges. In that example we fixed $d = 3$ and $w_f = 0$ and varied $q_1 = -1 + \Delta q$ and $q_2 = -1 - \Delta q$. For $\Delta q = 0$, the templates exactly neutralize the source density, and thus ET finds the exact location of the source points at $(x_1, x_2) = (1.50, -1.50)$. For moderate $\Delta q = 0.4$, the global minimum shifts toward $x = -d/2$ at $(x_1, x_2) = (0.88, -1.74)$, but $x_1 - x_2 = 2.62$ is still relatively close the source separation. However, for extreme $\Delta q = 0.8$ the local and global minima exchange roles and the minimum energy configuration corresponds to a bound state around $x = -d/2$ with $(x_1, x_2) = (-1.00, -1.90)$. With this extreme fluctuation, the source at $-d/2$ looks to ET very similar to a valid case of two overlapping tracks, and without further information ET cannot help being fooled.

This phase transition is clearly revealed in Fig.4 where the template separation at the global energy minimum is plotted as a function of $|q_2 - q_1|$ for fixed $q_1 = -0.3$ and different d. For $d > 3$ there is a clear discontinuity near $|q_2 - q_1| \approx 1$ showing how the local and global minima interchange when charge fluctuations exceed a critical value.

With this background we can understand the features of the curves showing the rms fluctuations of the template separation around the source separation in Fig.5. For each source separation d, the rms fluctuation

$$\Delta d \doteq (\langle (x_1 - x_2)^2 \rangle - \langle (x_1 - x_2) \rangle^2)^{\frac{1}{2}} \ , \tag{16}$$

was computed directly via numerical integration rather than gradient descent via

$$\langle (x_1 - x_2)^n \rangle = \int_{-1-\Delta q}^{-1+\Delta q} \frac{dq_1}{2\Delta q} \frac{dq_2}{2\Delta q} (x_1(q_1, q_2, d) - x_2(q_1, q_2, d))^n \ . \tag{17}$$

Assuming a uniform distribution of charge fluctuations for illustration.

In Fig. 5 we see that for small fluctuations $\Delta q/q = 0.1$, ET can resolve tracks separated by as little as 1/4 of the intrinsic source width. As $\Delta q/q$ increases to 50% ET can still resolve tracks separated by half their natural width, but a curious long tail develops at large d. For extreme fluctuations $\Delta q/q = 0.7$ there is an evident breakdown of the resolution at large separation. This simply reflects the phase transition to local bound states configurations shown in Figs.3 and 4. This is an unavoidable problem when the source density can fluctuate with high probability into one resembling true overlapping tracks.

The only solution to the above problem is to decrease the local fluctuation or increase in the amount of global information. The simplest solution is to increase the number of independent measurements of the source density. Including N rows of detectors, the total charge fluctuation $\delta q^2 \sim \delta q_0^2/N \to 0$ as $N \to \infty$. While the fluctuations, δq_0^2, on any given detector layer may be large, the net fluctuation on the combined source distribution can be made arbitrarily small. Of course a global

algorithm, such as ET, is required to take advantage of all the information the detector provides. In the example in Fig.5, if the fluctuation on a detector row is 70% then the resolution curve corresponding to the one labelled $\Delta q/q = 0.1$ is achieved by ET if 50 detector rows are used.

4 Numerical results

We turn next to a more realistic numerical example of tracking two ionization paths with a common vertex in a 2-D model of a TPC like detector with N pad rows in the z-direction. We assume for that the source charge density on row i can be expressed as

$$\rho_i^S(x) = -\sum_\alpha (1 - \delta q_{\alpha,i})\sigma(x - x_{\alpha i}) \ , \tag{18}$$

where $\delta q_{\alpha,i}$ is the charge fluctuation of track α on row i. For simplicity we limit the study to straight trajectories for which the intersection points can be parametrized as $x_{\alpha i} = i x_\alpha / N$, where x_α is the intersection point on row N. Curved trajectories and higher dimensions only increase the dimension of the template phase space and thus the number of coupled equations that must be solved without adding new insight into the problem. In fact higher dimensions simplify the problem since for a fixed multiplicity the mean ρ_{track} decreases with increasing dimensions.

In this example, we assume a histogram form for the source $\sigma(x)$ to simulate the image charge distributions on an array of pads in a TPC like detector [7]. All distances are measured in units of the pad width, Δx. Fig. 1. illustrates the source density in a $N = 20$ row detector for different track separations, d, as defined by the source separation on the row furthest from the common origin of the tracks. As our model of the response of the EOS/TPC/[7] we assumed that the source image charge distribution on pad i of row k is given by a clipped parabolic form:

$$\begin{aligned} \rho_{ik}^S &= (-1 + \Delta q_{1k})[(i\Delta x - k d_1/N)^2 - w^2]_> + \\ &\quad (-1 + \Delta q_{2k})[(i\Delta x - k d_2/N)^2 - w^2]_> \ , \end{aligned} \tag{19}$$

where $[f]_> = f\theta(f)$ and $w = 1.2$. The d_i denote the crossing points of the track on row $N = 20$ and are simply related to the opening angle of the tracks ($\theta = |\tan^{-1}(d_1/N) - \tan^{-1}(d_2/N)|$). For the template density we thus take

$$\rho_{ik}^T = [(i\Delta x - k x_1/N)^2 - w^2]_> + [(i\Delta x - k x_2/N)^2 - w^2]_> \ , \tag{20}$$

As in the example in the previous section the problem is to find x_1, x_2 as close as possible to d_1, d_2 given independent fluctuations of source charges $\Delta q_{\alpha k}$ on each detector row.

Aside from the use of a more realistic source density, this example is more challenging because the tracks converge at a common origin. Thus even for $d_1 - d_2 = 4$ as shown in Figs. 1,2 a large fraction of the detector rows respond to overlapping source distributions with $k(x_1 - x_2)/N \lesssim w$. Also the histogram form of the charge density implies that the potential V cannot be taken to have zero range as could be assumed in section 3.

The initial width of the potential is chosen to be close to half the detector width to insure that any arbitrary initial configuration (x_1, x_2) get attracted toward the mid point of the source density. Then slowly the width is decreased to $w = 1.2$ so that the system finds the global minimum. (As a technical note, in our numerical implementation of the ET line integral only pads intersecting the line *orthogonal* to a given template were actually taken into account.) The ET solutions for the examples in Fig.6 are shown by the solid lines.

To calculate the rms two track resolution in this example, we solved the coupled gradient descent equations for each source separation using 500 different initial source charge configurations, $\Delta q_{\alpha k}$, sampled from a uniform distribution from $-1 - \Delta q$ to $-1 + \Delta q$. The resulting average resolution, Δd, is shown in Fig. 6 for the case $\Delta q = 0.75$. The curves are labelled by the number of rows ΔN starting on row 20 toward the vertex which were taken into account in the analysis. The curve for $\Delta N = 1$ is similar to the one labelled $dq/q = 0.7$ in Fig. 5. The rapid rise of Δd for large d is due to the phase transition to bound states described in section 3 for extreme fluctuations. Note that in this case the local charge fluctuates by almost an order of magnitude with $q_{max}/q_{min} = 7$.

The important point to note in Fig. 6 is that the relative tracking error decreases rapidly as the number of rows (and thus the global information on the source density) increases. The saturation at high ΔN arises because on rows near the vertex the tracks are so close to each other that the limiting resolution as $d \to 0$ in Fig. 5 comes into play. Higher resolution can be achieved for fixed Δq only by adding detector rows further away from the vertex.

We conclude from these results that the ET algorithm can easily achieve sub-pad relative track resolution when applied to unprocessed data of the type expected in TPC detectors.

5 Summary

We have shown that Elastic Tracking is a powerful adaptive template matching algorithm that can be used to improve significantly existing multiple tracking capabilities. The important advantage of ET that we emphasized in this work was that no local preprocessing of the measured ionization distribution is required. Even with large fluctuations at the pad level, sub-pad multiple track resolution can be achieved when sufficiently many detector rows are introduced to measure the ionization density along the trajectories. The success of the method stems from its efficient utilization of the global information provided by the detector as well as the inclusion of the known physical constraints on the class of trajectories allowed in that detector. In the limit $N \to \infty$, ET converges to the exact solution for arbitrarily small track separations. For real detectors, ET can be used to squeeze out the last drop of information from the data to reduce the tracking errors to an absolute minimum.

In practical applications it may also be possible to develop a direct on-line hardware implementation of the ET method. For each template one processor is needed to evolve the gradient descent equations for that template in the mean field produced by

the measured source and the competing template distributions. A very small number of template phase space parameters need to be shared between the processors. The adiabatically evolving width of the effective ET potential function would be just one more shared parameter among all the units. The raw data would be piped in parallel to all processors. Such an on-line parallel approach would reduce greatly the need to store vast amounts of (uninteresting) ionization charge data. The ideal (gedanken) detector should output the physically interesting track phase space parameters rather than their intermediate representation in terms of complex ionization distributions. With the development of global pattern recognition algorithms such as ET and the rapid development of VLSI technology that could make massively parallel hardware implementations feasible, that ideal may not be so far out of reach.

Finally, we note that ET generalizes easily to any number of overlapping curved "tracks" of arbitrary dimension. In particular, it should prove useful in applications to multipion interferometry[13] where the premium is on achieving the highest discrimination power on very close tracks. The half pad two track resolution demonstrated in our numerical example significantly exceeds the three pad resolution imposed on conventional local algorithms that require data preprocessing. Our results on multiparticle tracking problems in [1] also showed that the utilization of known long range correlations in the sought after patterns is essential to enhance the tracking capability compared to even neural-network algorithms[11, 12] which also are global but utilize only few particle effective interactions. We conclude that Elastic Tracking should be a useful addition to the arsenal of techniques used in high energy and nuclear physics as well as in other fields to solve complex pattern recognition tasks.

Acknowledgements: We are grateful to Peter Jacobs for valuable discussions on tracking problems in TPC's. Discussions with D. Dong, G. Rai, H. H. Wieman, H.G. Ritter, J. Harris, M. K. Harlander and A. Poskanzer are also gratefully acknowledged.

A copy of the image or the source code can be obtained by sending mail to **harlan@physik.tu-muenchen.de** or **gyulassy@nsdssd.lbl.gov**.

References

[1] M. Gyulassy and M. Harlander, Computer Physics Communications 66 (1991) 31.

[2] J. Illingworth and J. Kitter, Computer Vision, Graphics, and Image Processing 44 (1988) 87.

[3] H. Grote, Rep. Prog. Phys. 50 (1987) 473.

[4] M. Regler and R. Frühwirth, in Proc. Advanced Study Institute on Techniques and Concepts in High Energy Physics, St. Croix 1988 (Plenum Publ. Corp., Rochester).

[5] R. Durbin and D. J. Willshaw, Nature 326 (1987) 689; W. S. Wong and C. A. Funka-Lea, IJCNN 1990 op cit, Vol III, p.799.

[6] A. Yuille, K. Honda, C. Peterson, "Particle Tracking by Deformable Templates", Proc. IEEE INNS/IJCNN, Vol. 1 (1991) 7, Harvard Robotics Lab Report 90-8 (90).

[7] G. Rai et al., IEEE Trans. on Nucl. Sci., 37 (1990) 56; H.G. Pugh et al, LBL-22314 (1986) preprint (unpublished).

[8] Proc. Second Workshop on Experiments and Detectors for RHIC, LBL-24604 (1988), CONF-870543; Proc. Third Workshop on Experiments and Detectors for RHIC, BNL (1990).

[9] K. Kadija, et al (STAR collab), LBL-31040 (1991) preprint.

[10] W.W.M. Allison and J.H.Cobb, Ann. Rev. Nucl. Part. Sci. 30 (1980) 253

[11] B. Denby, Comput. Phys. Commmun. 49 (1988) 429;
B. Denby and S. L. Linn, Comput. Phys. Commun. 56 (1990) 293;
B. Denby et al., IEEE Transactions on Nuclear Science 37 (1990) 248.

[12] C. Peterson, NIM A279 (1989) 537; Neural Networks 2 (1989) 475; LU-TP-89-1 (1989) Lund preprint.

[13] J.G. Cramer, "Mixed Charge" HBT Interferometry for Large Pion Sources, U.Washington Preprint April 1991

Figure Captions

Fig. 1 Examples of the ionization density in a 2D simulation of an ideal TPC like detector with 20 layers without local charge fluctuations. The cases of two overlapping tracks with a separation $d = 0.5$ on layer 20 and nonoverlapping tracks with $d = 4$ are shown. Top tick marks indicate location of crossing points of input tracks. The solid lines show the ET solution with a potential illustrated by the bell shaped curve on the center layer. Also an example with 3 overlapping tracks is shown.

Fig. 2 The same configurations as in Fig. 1 but in a more realistic detector with large local fluctuations of the ionization density ($dq/q = 0.75$).

Fig. 3 Examples (1D) of the ET template density, $\rho_T(x)$ minimizing the effective energy in the field produced by Gaussian sources, $\rho_S(x)$, separated by $d = 3$. The short dashed curve illustrates the phase transition to a local bound state when the charge fluctuations on a source exceed a critical value.

Fig. 4 The template separation at the global minimum for fixed source separations $d = 1, 3, 5, 7$, as a function of the charge fluctuation, q_2, on source 2 in the 1D example of section 3. Fixed is $q_1 = -0.3$ and template charges $q_T = 1$. The phase transition for $\Delta q \sim 1$ for large separations is obvious.

Fig. 5 The rms resolution on the source separation in the 1D example as a function of the source separation d. Curves for different ranges of uniform charge fluctuations with $-1 - dq/q \leq q_i \leq -1 + dq/q$ are shown.

Fig. 6 Relative two track resolution in pad units as a function of source separation for the 2-D example in Fig. 2 and for large local charge fluctuations $dq/q = 0.75$. ΔN refers to the number of detector rows below and including row 20 that were included in the analysis.

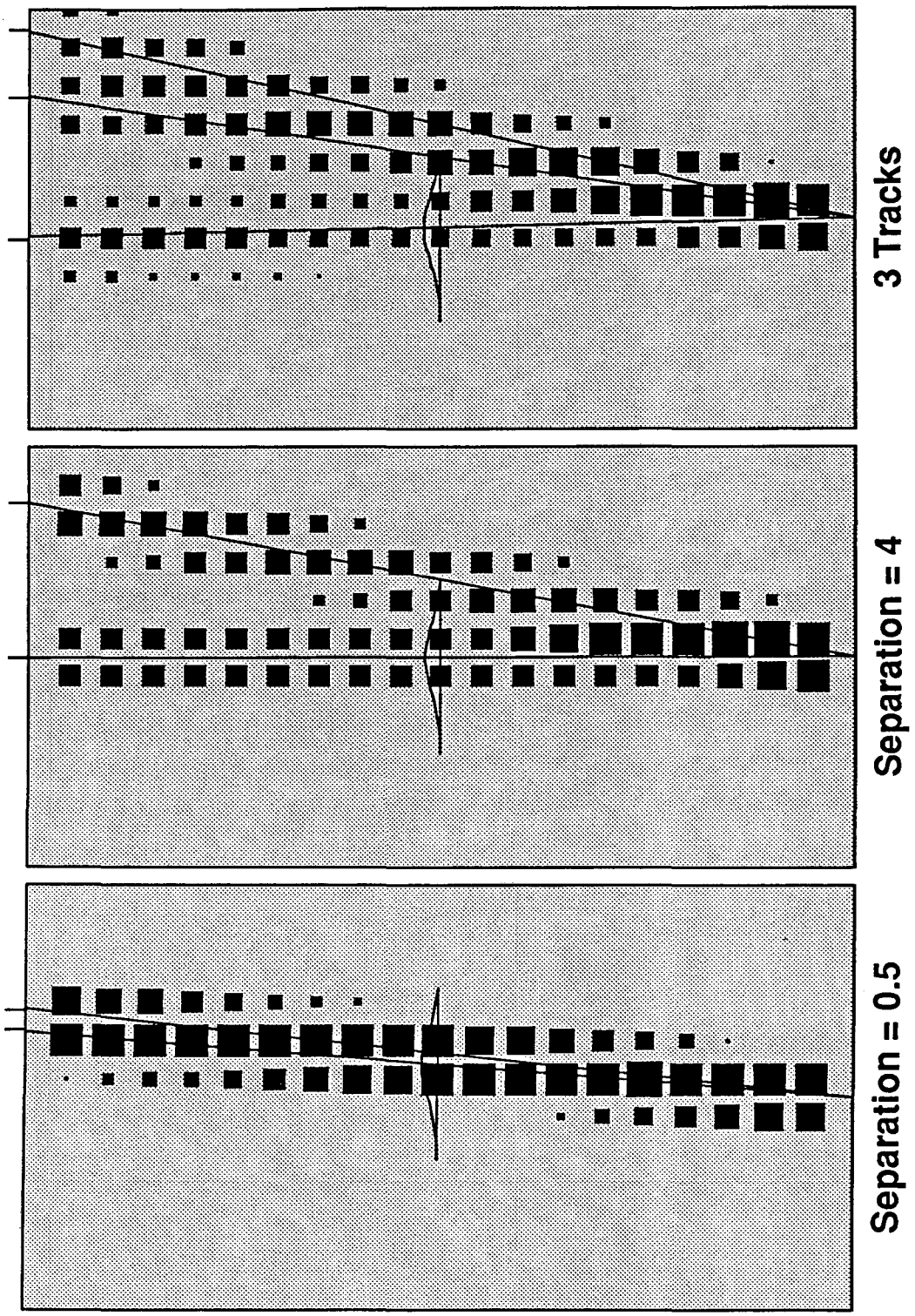
Separation = 0.5
Separation = 4
3 Tracks

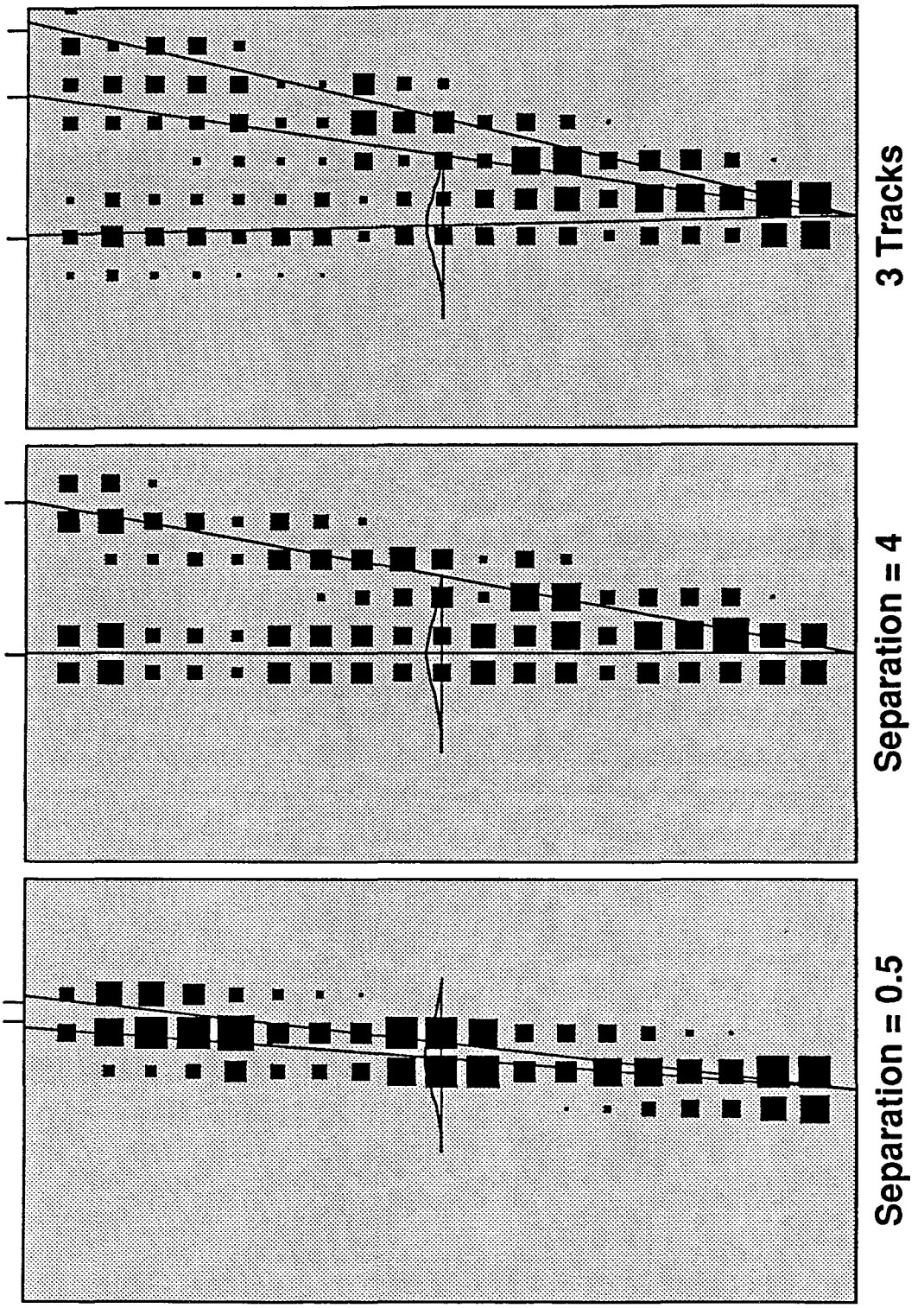
Separation = 0.5
Separation = 4
3 Tracks

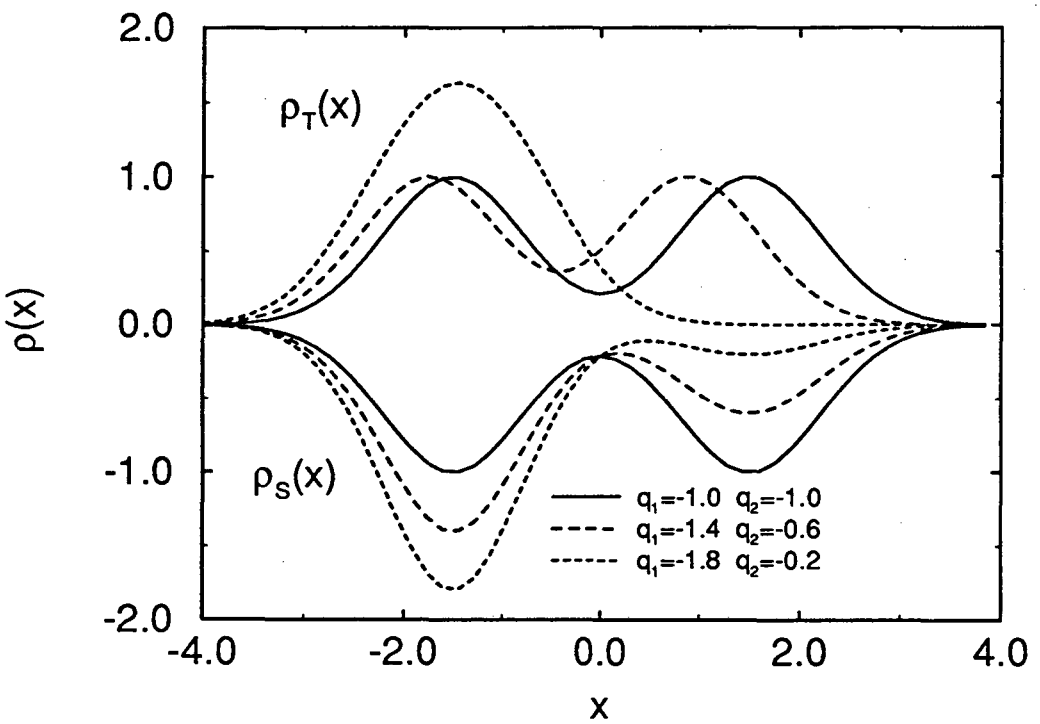
2.0
1.0
0.0
-1.0
-2.0
ρ(x)
ρT(x)
ρS(x)
q1=-1.0 q2=-1.0
q1=-1.4 q2=-0.6
q1=-1.8 q2=-0.2
-4.0
-2.0
0.0
2.0
4.0
x

Figure 3:

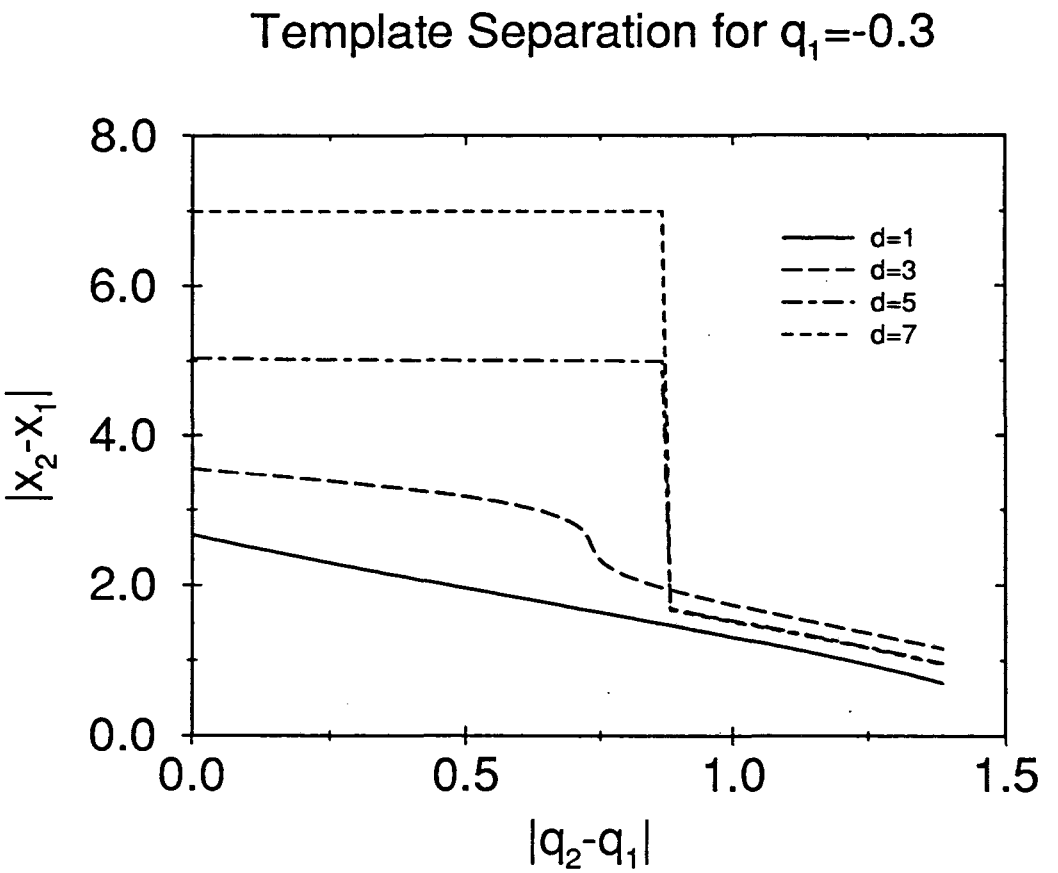
Template Separation for q_1=-0.3
8.0
6.0
4.0
2.0
0.0
0.0
0.5
1.0
1.5
$|x_2-x_1|$
$|q_2-q_1|$
d=1
d=3
d=5
d=7

Figure 4:

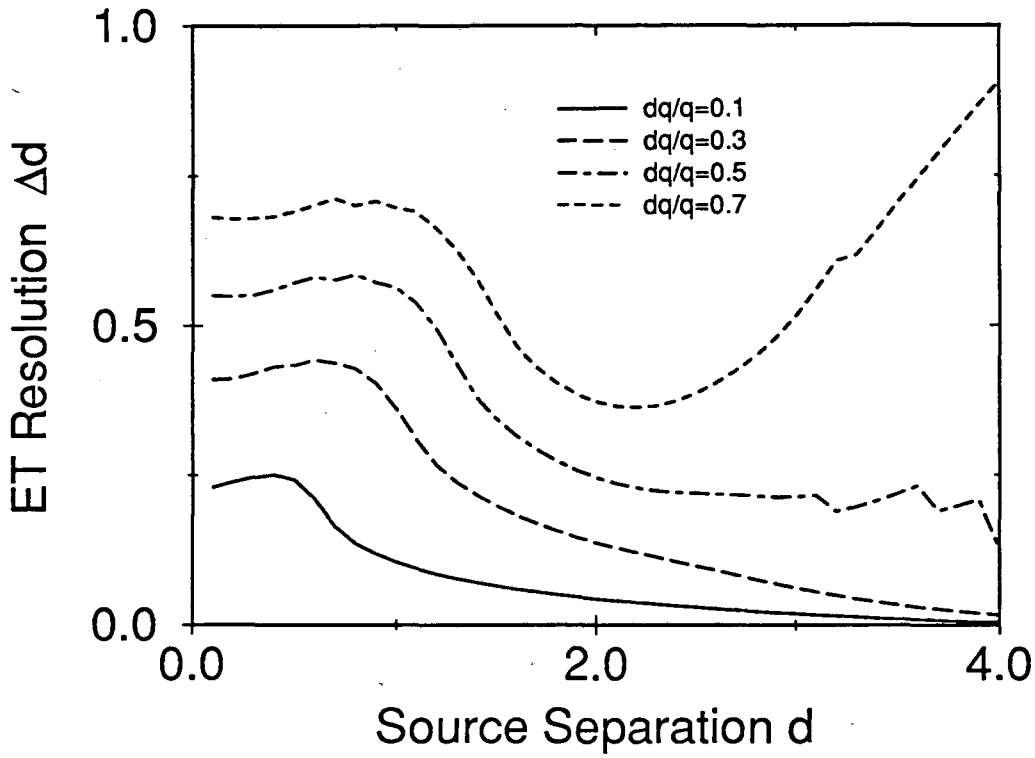
1.0
0.5
0.0
0.0
2.0
4.0
ET Resolution Δd
Source Separation d
dq/q=0.1
dq/q=0.3
dq/q=0.5
dq/q=0.7

Figure 5:

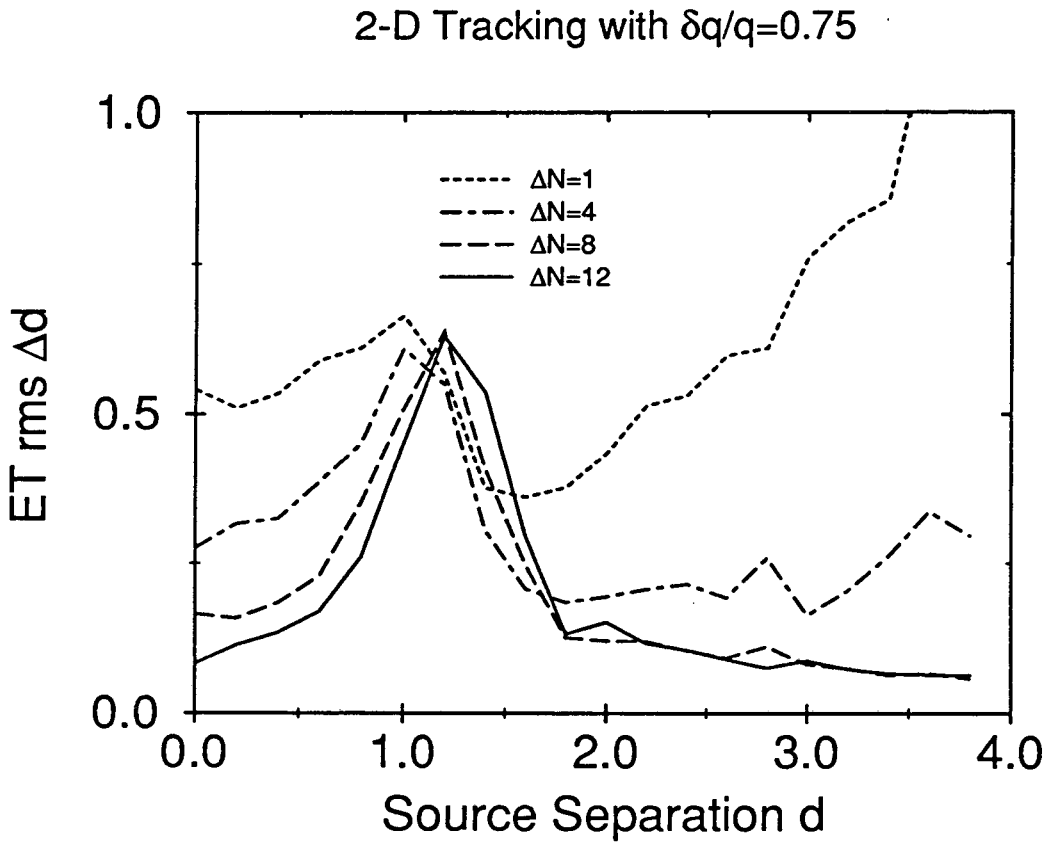
2-D Tracking with δq/q=0.75
ΔN=1
ΔN=4
ΔN=8
ΔN=12
ET rms Δd
1.0
0.5
0.0
0.0
1.0
2.0
3.0
4.0
Source Separation d

Figure 6:

LAWRENCE BERKELEY LABORATORY
UNIVERSITY OF CALIFORNIA
INFORMATION RESOURCES DEPARTMENT
BERKELEY, CALIFORNIA 94720